AD_____

Award Number: W81XWH-07-2-0020

TITLE: Molecular Evolution of Human PON to Design Enhanced Catalytic Efficiency for Hydrolysis of Nerve Agents

PRINCIPAL INVESTIGATOR: Dan Tawfik, Ph.D.
Joel L. Sussman, Ph.D.

CONTRACTING ORGANIZATION: Weizmann Institute of Science
Rehovot 76100 ISRAEL

REPORT DATE: December 2011

TYPE OF REPORT: Final

PREPARED FOR: U.S. Army Medical Research and Materiel Command
Fort Detrick, Maryland 21702-5012

REPORT DOCUMENTATION PAGE

Form Approved
OMB No. 0704-0188

1. REPORT DATE	2. REPORT TYPE	3. DATES COVERED
December 2011	Final	29 January 2007 – 23 November 2011

4. TITLE AND SUBTITLE

Molecular Evolution of Human PON to Design Enhanced Catalytic Efficiency for Hydrolysis of Nerve Agents

5a. CONTRACT NUMBER

5b. GRANT NUMBER
W81XWH-07-2-0020

5c. PROGRAM ELEMENT NUMBER

6. AUTHOR(S)

Dr. Dan Tawfik, Ph.D.
Dr. Joel L. Sussman, PhD

E-Mail: Dan.Tawfik@weizmann.ac.il

5d. PROJECT NUMBER

5e. TASK NUMBER

5f. WORK UNIT NUMBER

7. PERFORMING ORGANIZATION NAME(S) AND ADDRESS(ES)

Weizmann Institute of Science
Rehovot 76100 ISRAEL

8. PERFORMING ORGANIZATION REPORT NUMBER

9. SPONSORING / MONITORING AGENCY NAME(S) AND ADDRESS(ES)
U.S. Army Medical Research and Materiel Command
Fort Detrick, Maryland 21702-5012

10. SPONSOR/MONITOR'S ACRONYM(S)

11. SPONSOR/MONITOR'S REPORT NUMBER(S)

12. DISTRIBUTION / AVAILABILITY STATEMENT
Approved for Public Release; Distribution Unlimited

13. SUPPLEMENTARY NOTES

14. ABSTRACT

Project Summary: A technology was developed to identify proteins capable of intercepting both existing and emerging organophosphate-based chemical warfare nerve agents (CWNA). The 5 years of performance under this project have demonstrated the potential of directed evolution, combining random and designed mutations based on 3D structures, to generate mutants of a recombinant mammalian PON1 (rePON1) with catalytic proficiency well above that of the wild type (wt)1-3. We have evolved mutants that hydrolyze >105-fold faster the toxic isomers of the coumarin-based nerve agent surrogates, when compared to wt rePON1 and human PON1. The kcat/Km values for these variants when reacting with G-type CWNA are as high as 2-5x107 M-1min-1, a value that approaches the theoretical estimated minimal requirement for efficient prophylactic protection at a reasonable protein dose (~50 mg/70 kg). The most advanced mutants were evolved to completely reverse the stereo-preference of PON1 from the non-toxic to the toxic isomers of racemic nerve agents. PON1 variants evolved by selection with VX are capable of hydrolyzing the toxic isomer of VX >75,000-fold faster than the wt enzyme. Preliminary in vivo evaluation (in guinea pigs) at ICD, Aberdeen Proving Ground MD, demonstrated the ability of several PON1 variants to confer protection in a catalytic manner against multiple LD50 doses of all G-type nerve agents at protein dose of 1 mg/kg. Relevance: This technology permits rapid discovery of pretreatment and post challenge therapeutic drugs against existing and emerging CWNA threats at low protein doses. Existing libraries will shorten the time from emergence of a new CWNA threat to identification of potential counter-measures to a few days or weeks.

15. SUBJECT TERMS
Directed evolution, X-ray crystallography, organophosphates & bioscavangers

16. SECURITY CLASSIFICATION OF:			17. LIMITATION OF ABSTRACT	18. NUMBER OF PAGES	19a. NAME OF RESPONSIBLE PERSON
a. REPORT	b. ABSTRACT	c. THIS PAGE			USAMRMC
U	U	U	UU	37	19b. TELEPHONE NUMBER *(include area code)*

Table of Contents

Introduction

The long-term objective of this effort is to develop a generic gene shuffling-based technology to rapidly screen libraries of 10^{10} proteins/peptides encoded by DNA libraries, for identifying biomolecules that can intercept both existing and emerging organophosphate-based chemical warfare nerve agents (CWNAs). Enzymes identified in these screens should be capable of catalytically neutralizing the target agent under physiological conditions, thereby providing a basis for development of a new generation of therapeutic agents against CWNAs. The major milestone was to integrate established components of enhanced molecular evolution techniques so as to provide a means of miniaturizing existing low-throughput assays, thereby dramatically increasing both sensitivity and throughput. The expressed biomolecules were allowed to intercept the CWNA, preventing interaction with its target (*viz.* AChE), and genes code for effective interceptors were isolated. Uniquely, this screen is for directly detoxifying the CWNA, not simply for binding it, thus allowing identification of biomolecules that prevent its action by degradation at the desired rate. This technology was envisaged to provide rapid discovery of pretreatment and post-challenge therapeutic drugs against existing and emerging CWNA threats, and thus to shorten the time from emergence of a threat to identification of potential counter-measures to a few days or weeks.

G- and V-type type nerve agents: tabun (GA), sarin (GB), soman (GD), cyclosarin (GF) and VX **(Figure 1a),** are highly toxic organophosphates (OPs) that penetrate the body both by inhalation and skin absorption[4]. They contain a chiral phosphorous center, whose optical isomers differ in their toxicity. The S_P isomers of GB, GD, and GF inhibit acetylcholinesterase (AChE) >1000 fold faster than their respective R_P isomers and are considered to be much more toxic[5]. The S_P isomer of VX inhibits AChE approximately 100-fold faster than the R_P enantiomer. For GD, in addition to its chiral phosphorous, a chiral carbon center (**Figure 1a**) produces 4 diastereo-isomers: S_PS_C, S_PR_C, R_PS_C and R_PR_C. However, since the chirality of the phosphorous in GD has a much greater influence on AChE toxicity than the chirality of its alpha carbon[6], only two of its isomers are considered toxic: S_PS_C and S_PR_C. In the case of GA, which contains a cyanide in place of a fluoride **(Figure 1a)**, nomenclature conventions dictate an R_P configuration for its toxic isomer. Following their entrance, G-agents bind to and inhibit AChE, thus causing a cholinergic crisis that may result in respiratory failure and death[7]. Current treatments of OP intoxication are symptomatic and do not act to reduce blood OP levels and, thereby, to prevent AChE inhibition[8,9]**.** A better treatment strategy might be achieved by employing OP hydrolyzing enzymes as prophylactic drugs that would promote rapid OP degradation *in-vivo*[10-12]. Unfortunately, most OP-hydrolyzing enzymes isolated thus far show preference towards the non-toxic isomers of nerve agents, and hydrolyze the toxic isomers with low catalytic efficiencies[13,14]**.** Until this project was initiated, there were no available enzymes capable of hydrolyzing the toxic isomers of nerve agents at a rate that would permit them to offer effective prophylactic protection at low protein doses (< 50mg/70kg). Notably, treatment with the most advanced non-catalytic enzyme scavenger, human butyrylcholinesterase, requires the administration of a dose of several hundred milligrams per person in order to confer reasonable protection against nerve agents[15].

PON1 is a mammalian lactonase that exhibits a promiscuous OP-hydrolyzing activity[3,16]. It resides on cholesterol-carrying HDL blood particles where it plays a role in drug metabolism and in the prevention of atherosclerosis[17-19]. Human PON1, and the other mammalian PONs, hydrolyze G-agents at low catalytic efficiencies and react primarily with their less toxic R_P isomers[20]. Using directed evolution we obtained a recombinant PON1 (rePON1) variant, G3C9,

which expressed well in soluble form in *E coli*, that was selected as the wt lead variant for directed evolution.

Over the last 5 years of performance in the framework of this project, we have demonstrated the potential of directed evolution, combining random and designed mutations based on 3D structures, to generate mutants of a recombinant mammalian PON1 (rePON1) with catalytic proficiency well above that of the wild type[1-3]. We have evolved mutants that hydrolyze the toxic isomers of the coumarin-based nerve agent surrogates $>10^5$-fold faster than rePON1 and human PON1. We have also developed a safe *in situ* protocol for generating the corresponding fluoridates (*i.e.,* the threat G agents), and showed that k_{cat}/K_m values for these variants are as high as $2\text{-}5x10^7$ $M^{-1}min^{-1}$, values approaching the theoretical estimated minimal requirement for efficient prophylactic protection at reasonable doses (~50 mg/70 kg) without the need for post-exposure therapy. In addition, we have shown that PON1 variants evolved by selection with VX are capable of hydrolyzing V-type agents, and anticipate that the current libraries will be further developed by use of directed evolution to evolve one or more variants that will be qualifie as V-type agent antidotes. It seems likely that not more than two PON1 variants will be required to provide broad-spectrum protection against all currently prevalent nerve agents.

Body

I. Specific Aims

1. The development of high-throughput-assays for OP hydrolase variants exhibiting high specificity factors and turnover.

2. Provision of proof-of-concept for the proposed core technology employing directed evolution of new recombinant PON and AChE variants.

3. Isolation of interceptors for G- and V-type nerve agents, and expression in soluble form.

4. Design, generation and selection of 2nd generation libraries for V- and G-type agents.

5. Large-scale production of selected enzyme candidates, and their kinetic, structural and pharmacological evaluation

6. Establishment of “off-the-shelf” libraries for rapid identification of antidotes against emerging future threats

II. Significance to the goals of Counter ACT

The proposed approach opens new opportunities for rapid identification, characterization and implementation of novel countermeasures against CW agents. It will significantly decrease the time interval between the appearance of a new threat and the discovery of potential antidotes to counteract it. The major benefits will be one or more products capable of efficient catalytic hydrolysis of G- and V-type nerve agents, as well as of gene libraries derived from existing enzymes that can be used “off-the-shelf” to isolate new protein variants for almost any nerve agent or toxic industrial chemical serving as a target for the screen.

III. Detailed Tasks - Performance and accomplishments.

A. Generation of the round zero library of G-type CWNA hydrolyzing variants[1]:

We used a recombinant variant dubbed rePON1-G3C9 (referred to as rePON1 in the following) that, unlike human PON1, is expressed in soluble and functional form in *E. coli*. Its amino acid sequence is 94% and 85% identical to rabbit and human PON1s, respectively[2]. The enzymatic specificity of rePON1 is essentially identical to that of human PON1, yet its stability is much improved, and its *in vivo* applicability and efficacy have been confirmed[21]. For safety and for facile detection, we initially used fluorogenic coumarin analogues (Figure 1b), including CMP-coumarin that inhibits AChE with a k_i that is 20-40 fold lower than cyclosarin itself (depending on the source of AChE)[20].

We earlier isolated several variants of rePON1 with enhanced activity towards a racemic mixture of CMP-Coumarin by screening 'neutral drift' libraries of rePON1 (e.g. 1G3, 2G9)[22]. The most active variant was 3B3, which had ~250-fold higher catalytic efficiency (k_{cat}/K_m $20x10^6$ $M^{-1}min^{-1}$) compared to the wild-type-like rePON1 (k_{cat}/K_m $0.08x10^6$ $M^{-1}min^{-1}$). Although hydrolysis by rePON1-3B3 was restricted to the R_P isomer (not shown), we could use its high catalytic efficiency and R_P-stereoselectivity to isolate the S_P isomers of CMP-coumarin and IMP-coumarin from the corresponding racemates, and apply them in subsequent screens. We also identified low activity of H115W and V346A rePON1 mutants towards S_P-CMP-coumarin[20]. However, their activity with S_P-CMP-coumarin was too low for detection under library screening conditions. We therefore used for the initial rounds of screening the coumarin analog of sarin (IMP-coumarin), a less bulky G-agent surrogate whose S_P isomer is more reactive with PON1 (**Table 1**).

Random mutagenesis of rePON1-H115W-V346A, followed by screening of the resulting library in 96-well plates with S_P-IMP-coumarin, yielded several improved variants that typically carried one mutation in addition to H115W and V346A. A second round of mutagenesis and screening with S_P-IMP-coumarin led to isolation of variants in which the V346A mutation was removed and the H115W and F222S mutations dominated. As the evolving variants became more reactive towards the S_P isomer, the 3rd generation library could be screened with both S_P-IMP- and S_P-CMP-coumarin. Indeed, this round resulted in several variants with improved activities towards S_P-CMP-coumarin (*e.g.*, 3A7, 8C8; **Table 2**). However, since the 4th round of mutagenesis and screening yielded no further improvements, we designed a structure-based targeted library and subjected it to high-throughput screening (>10^6 variants per run) by FACS sorting[23,24], as described below.

The targeted substitutions library was based on PON1's active-site structure. In particular, a recently obtained crystal structure of the re-G3C9-H115W indicated movements of several side-chains in response to this mutation, including those of residues 69 and 134, that are in direct contact with W115, and of the more remote residues 346, 347 and 348 (Ben-David *et al.* unpublished data). We therefore generated a library by randomizing these positions and those of residues 115 and 222 that had been found to be mutated in all active variants of the 3rd round (**Table 3**). We applied an oligo spiking strategy that incorporated the randomizing oligos onto re-PON1-H115W in a combinatorial manner, so that each library variant carried on average 4 mutated positions[25]. Due to the intense level of mutagenesis, and the targeting of the active site, the libraries consisted mostly of inactive variants. To purge inactive library clones, we employed

[1] For experimental details and additional documented results please refer to: Gupta *et al* (2011) *Nat Chem Biol*, **7**, 120-125 (+ Supplementary Material)

a high-throughput FACS screen using a fluorogenic phosphotriester dubbed DEPCyC, whose susceptibility was found to correlate well with the activity on S_P-CMP-coumarin[20]. *E. coli* cells transformed with the plasmid library were compartmentalized in water-in-oil emulsion droplets. The fluorogenic substrate was added, and the primary emulsion droplets were converted to double-emulsion droplets that were sorted by FACS. Cells in isolated droplets were plated, picked, and assayed in 96-well plates for S_P-CMP-coumarin activity.

The most active variants isolated from this 5th round carried mutations L69G/A and H134R, in addition to H115W and F222S that had appeared in earlier rounds. These variants were shuffled, together with random mutagenesis at low rates (~1.7 amino acid exchanges per gene), and the resulting 6th round library was sorted by FACS, and then screened in 96-well plates. The most improved variants carried five key mutations: L69G, H115W, H134R, F222S and T332S (**Table 4**). The best variant, 3D8 exhibited a k_{cat}/K_m value of $1.2x10^7$ $M^{-1}min^{-1}$ with S_P-CMP-coumarin. Furthermore, 3D8 and other 6th round variants exhibited similar rates with both the S_P and R_P isomers as indicated by the complete hydrolysis of the racemic CMP-coumarin with monophasic kinetics (**Fig. 2**).

Along with selection of variants displaying higher rates, we decreased the concentration of the CMP-coumarin substrate so as to permit isolation of variants with improved K_m as well as k_{cat}. However, to be able to screen at concentrations that correspond to the very low toxic concentrations of cyclosarin *in vivo* (~1 μM)[4,15], and for variants that efficiently degrade cyclosarin itself, we developed a screen based on monitoring the rescue of AChE, the OP's physiological target. AChE was added to crude bacterial lysates expressing the library PON1 variants. The OP was added, and the residual activity of AChE was subsequently measured using a chromogenic assay to indicate the level of OP degradation by the tested variant. The FACS sorted 6th round library was re-screened in 96-well plates using the AChE assay, and 1 μM racemic CMP-coumarin. We screened 730 randomly-picked colonies, and isolated 13 variants that were improved by 2-12 fold relative to 3D8.

Although at this stage we had identified variants that exhibited sufficiently high catalytic proficiency, these had been selected and tested with coumarin surrogates. The fluoride leaving group of the actual threat agents differs substantially from coumarin (**Fig. 1**) – inasmuch as fluoride is both more reactive and much smaller. However, the toxicity of nerve agents prevents their use in ordinary labs. We therefore developed a non-hazardous screening protocol based on CMP-F generated *in situ*, in dilute aqueous solution, by replacing the coumarin leaving group of CMP-coumarin with fluoride. This exchange was spectroscopically monitored by following the release of the coumarin in the presence of NaF. The inhibition of *Tc*AChE by CMP-F thus generated *in situ* proceeded 40-fold faster than with S_P-CMP-coumarin, with the expected k_i of $1.3x10^9$ $M^{-1}min^{-1}$. Using the *in situ* generated CMP-F, we measured the k_{cat}/K_m values of the evolved variants under pseudo-first-order conditions (CMP-F ≤50 nM, well under a likely K_m). Encouragingly, the activities with the coumarin and fluoridate S_P isomers were comparable, and at least three variants (0C9, 2D8, 1A4) exhibited k_{cat}/K_m values of $\geq 10^7$ $M^{-1}min^{-1}$ with CMP-F (**Table 5**). The AChE protection assays thus confirmed the ability of the evolved variants to protect AChE from cyclosarin *in vitro*, and validated the coumarin analogues as faithful surrogates of the actual G-agents. The assay also confirmed that the starting point, rePON1-G3C9 is much more active towards CMP-F than towards CMP-coumarin (**Table 2**), as is human PON1[26], although the k_{cat}/K_m (~10^5 $M^{-1}min^{-1}$) is >100-fold too low for *in vivo* detoxification using reasonable amounts of enzyme.

The evolved variants were sufficiently active to permit library screens using the *in situ* generated agent. This approach is highly attractive, since the assay of AChE protection against the actual threat agent mimics the *in vivo* protection challenge whereby the catalytic scavenger must be sufficiently active to intercept the threat agent before the latter reacts with AChE. We therefore re-screened the 13 most improved variants from the last round, using CMP-F at the expected plasma concentration for $1xLD_{50}$ exposure (1 μM). Nine variants exhibited improved activities relative to 3D8. Of these, 3 variants (4E9, 5F3 and 6A3) exhibited the highest specific activity upon determination of the amount of soluble expressed protein. Following sequencing and protein purification, we identified 4E9 as the most active variant with both S_P-CMP-coumarin and S_P-CMP-F ($k_{cat}/K_m = 2.23x10^7\ M^{-1}min^{-1}$, and $1.7x10^7\ M^{-1}min^{-1}$, respectively).

B. Generation of advanced PON1s hydrolyzing G-type nerve agents

We generated gene libraries derived from the lead 2D8 of round zero above (**Table 4**) using structure-guided targeted mutagenesis. The 3D structure of 2D8 copied into the G2E6 scaffold **(Fig. 3)** revealed a flexible loop that covers the active site. Replacement of residues that were already fixed in 2D8 enabled us to generate smaller and more focused libraries that could be screened by our low-throughput 96-well plate screen. Several strategies were applied for the generation of advanced mutant libraries beyond round zero, as detailed below.

Strategy 1: Targeted diversification of active-site residues

Examination and comparison the structures of wt rePON1 (PDB code 1V04[3]) itself, of rePON1 in complex with the inhibitor 2-hydroxyquinone (PDB code 3SRG[27]), and of a docking model of rePON1 with the OP pesticide paraoxon[27], pointed to active-site positions that could affect OP binding and hydrolysis (*e.g.*, residues 70, 71, 196, 240 and 292). We also assumed that the activity of evolved variants could be further optimized by reexamining the mutagenesis of active-site residues that were substituted in the earlier rounds of directed evolution towards GF hydrolysis (*e.g.*, positions 69, 115, 134). We constructed the library by spiking mutations in these 8 active-site positions into the 2D8 gene in a combinatorial manner using the ISOR method[25]. In general, residues were mutated to amino acids with similar physico-chemical properties although more drastic changes were also included (e.g. Gly69Leu/Val/Ile/Ser). Sequencing of randomly selected clones revealed that the unselected library contained an average of 4 mutations per clone, with each clone exhibiting a different mutational composition. This round 1 library was then screened with *in-situ* generated GD and GB, using the AChE inhibition assay. This assay measures the ability of PON1 variants to prevent loss of AChE activity by rapidly hydrolyzing the toxic isomer of the added OP.

By the end of round 1 (see **Table 6a**) all improved variants had acquired mutations at two positions, 69 and 115, which had previously been mutated to improve GF hydrolysis[1]. Upon selection towards a broader range of G-agents, these residues changed again. In addition, improved variants had acquired a few more mutations, primarily at positions 70, 71, 196, 240 or 292. The changes in residues 69 and 115 led us to explore the re-optimization of another key active-site residue, 222, whose mutation to Ser had led to increased GF hydrolysis[1]. Residue Ser222 was therefore targeted for mutagenesis in the 2nd round library that was screened for GB, GD and GF neutralization (**Table 6b**). We speculated that mutations to hydrophobic residues (Leu, Val, Ile, Met) or to Cys might be beneficial. Indeed, 96% (24/25) of improved clones from the 2nd round library were mutated at position 222, mostly to Met (17/24).

In the 3rd round library (**Table 6b**), we targeted various residues whose side-chains are involved in structuring the top of PON1's active-site cleft. These included residues 50, 197, 291, 294, 346, 347 and 348. In addition, we retargeted positions 196 and 292 that had been explored during the generation of the 1st-round library, but acquired no mutations**.** On average, each clone of the naïve (*i.e.,* unselected) 3rd round library contained 2±1 substitutions at the targeted positions. Following screening with GB and GD, we obtained 18 improved clones in which positions 197 and 291 were primarily mutated, *i.e.*, 22% (4/18) and 44% (8/18) of selected clones, respectively. Some positions did not accept any mutations (196, 294, 346, 347, 348), and others were mutated in single clones (50, 292).

Strategy 2: Random shuffling of improved variants

Shuffling of selected variants can combine beneficial mutations that were acquired in separate variants, or eliminate deleterious mutations from individual variants. In particular, since the mutational diversity in our libraries was large compared to the number of clones screened (screening covered between 0.07 to $4x10^{-4}$ of the theoretical library diversity), most active variants isolated exhibited different mutational compositions. In fact, shuffling of improved variants was applied in every round in conjunction with the ISOR protocol[25] that was used to introduce the targeted mutations. For the round 4 library, however, shuffling was applied on its own with no spiking of targeted mutations.

Strategy 3: Targeted mutagenesis of the flexible active-site loop

PON1's longest active site loop (residues 70-78) is highly flexible, and is not observed in the crystal structures of wild-type-like rePON1 in its uncomplexed form[3]. However, upon binding of the lactam inhibitor, 2-hydroxyquinoline (2HQ), the loop became structured, thus completing the active-site cleft in the crystal structure[27]. Residues Tyr71 and Ile74, in particular, comprise part of the active-site wall, and make contact with the 2HQ. In addition, the loop configuration, and the position of Tyr71 in particular, seem to vary between different substrates[27]. Indeed, mutations in positions 70 (Lys to Asn or Gln) and 71 (Tyr to Phe or Ile) appeared in many improved clones from round 2. During round 3, we therefore designed a library devoted to examining the effects of active-site loop mutations. Specifically, given the very small size of the fluoride-leaving group of G-agents, we explored loop mutations that introduced large side-chains, such as Trp, Phe and Tyr that might reduce the active-site volume and improve substrate binding. We also attempted to affect the loop's configuration by mutating its residues to Gly and Pro. Since we introduced amino-acid substitutions using short oligonucleotides (21-29 bp), most substitutions were mutually exclusive, and each clone carried, on average, only one loop mutation.

Strategy 4: Introduction of ancestral mutations.

Ancestral mutations, *i.e.*, substitutions at residues that have appeared along the evolutionary history of a given protein, have been shown to be powerful modulators of a protein's stability and function[28-30]. A library based on active-site substitutions borrowed from the predicted ancestors of vertebrate PONs has been constructed[28]. This library was screened for OP-hydrolyzing activities using CMP-coumarin, and several ancestral mutations that were able to increase this activity in variants were identified[28]. We included these mutations (Leu55Ile, Ile74Leu, Asp136His, Pro189Gly) together with similar ones (55Met/Val, 136Gln, 189Ser) in the round 3 library, at an average frequency of. 0.5 mutations per gene in the unselected library.

Table 6b summarizes the results of four rounds of directed evolution starting from lead variant 2D8, and screening for GB and GD hydrolysis. Screening ~2000 variants in round 1, we identified 21 clones that were improved up to 4-fold with GB, and up to 5-fold with GD, relative to 2D8, in crude cell lysates. The two most active variants with GD, 5H8 and PG11, were purified and characterized. We found improvements of 21- and 4-fold in the catalytic activity of the best variant, PG11, with the two toxic isomers of GD relative to the starting variant, 2D8. However, its activity with GF was reduced 2.3-fold relative to 2D8, and no improvement in GB activity occurred. The two best variants shared the same 4 active-site mutations: Leu69Val, His134Arg, Phe222Ser and Thr332Ser, but differed at position 115: 5H8 acquired a Val and PG11 an Ala. While mutations Phe222Ser and Thr332Ser were already present in the parent variant, 2D8, the mutations in positions 69, 115 and 134 were selected from the substitution library of round 1.

For the 2nd round, we constructed a substitution library that explored various substitutions at position 222, whilst shuffling the 10 most active clones found in round 1. The resulting library was screened on GD and GB, as well as on GF. The latter was included to eliminate variants that exhibit reduced activity with GF, as observed with variants isolated from the 1st round. Screening of ~1000 clones we found 39 variants that were improved up to 4-fold towards GB, 2-fold towards GD and 4-fold towards GF relative to the best variants of round 1**.** Sequencing revealed 25 unique variants and 14 duplicated variants. Following more detailed screens (at different agent concentrations), we selected the 6 most active variants, purified and characterized them. All purified variants had improved catalytic rates up to 7- and 193-fold towards the toxic isomers of GD, and up to 5-fold towards GB, relative to the starting variant, 2D8. Their activities towards GF were improved relative to variants from round 1, and they became similar to that of 2D8. All round 2 variants contained three mutations: Leu69Val, His134Arg and Thr332Ser, and all but one contained also the Phe222Met mutation. The greatest variability was seen at position 115, where either Ala, Leu or Val were observed. While no attempt to introduce random mutations during library construction was made, the PCRs applied for library making produced random mutations such as Phe64Leu or Asp309Gly, that were retained in certain improved variants. By round 2, the most improved variants we isolated reached the targeted catalytic efficiency of $\geq 10^7$ [M^{-1} min^{-1}] for GD and GF, but were still 10-fold lower in activity towards GB. The best round 2 variant, VII-D11, hydrolyzed the two toxic isomers of GD with equally high rates ($2.9x10^7$ [M^{-1} min^{-1}].

During the 3rd round, two libraries were constructed and screened for variants with increased activities using GD and GB. The libraries were made by shuffling the 7 most active variants from round 2, together with oligonucleotides encoding for specific mutations in PON1's active site and flexible active-site loop. The construction of two such libraries enabled us to screen a larger diversity of mutations in separate regions of the enzyme. Library #1 introduced mutations in active-site positions that had not yet been mutated in the previous rounds and in second shell positions around the active site, as well as ancestral substitutions. Library #2 included mutations in the active-site loop. Screening 400 variants from each library with GD and GB identified a total of 18 improved clones. All selected clones were improved for GB but only 67% (12/18) were also improved for GD. Most of the improved variants originated from Library #1 (73%, 13/18), and the improvements for GB (1.6-4-fold) were also greater than for GD (1.1-1.6 fold). Sequencing indicated that 55% (10/18) of the selected variants contained at least one ancestral mutation (Leu55Ile, or Asp136His) and 28% (5/18) contained two ancestral mutations. In addition to these ancestral mutations, the active-site mutation Ile291Leu became abundant in

selected clones (39%, 7/18). Certain mutations introduced in earlier rounds, such as His134Arg and Phe222Met, were fixed (*i.e.*, appeared in all selected clones) and others, such as Leu69Val and His115Ala, were nearly fixed (90%, 16/18). We purified and characterized the four most improved variants from this round**.** The catalytic efficiencies of these variants were improved up to 11- and 293-fold for the two toxic isomers of GD, and up to 17-fold for GB, relative to 2D8, our starting variant. A small 3-fold improvement was found for GF hydrolysis. The catalytic efficiency of our most improved variant, 1-I-F11, with GB ($3.9x10^6$ M^{-1} min^{-1}) was improved >3-fold relative to the best round 2 variant, but was still 2.5-fold lower than our goal.

The round 4 library was constructed by shuffling the 18 most improved variants from round 3 with the aim of recombining beneficial mutations identified in separate variants. We screened 700 library clones using GB and GD, and isolated 22 improved variants of which 18 were unique. Of these, 66% (12/18) were improved mostly for GB, and 33% (6/18) were improved also for GD. In addition to the mutations fixed in earlier rounds, all selected Round 4 variants now contained the mutation His115Ala, and most variants also carried Leu55Ile (55%, 10/18) and/or Ile291Leu (83%, 15/18). We purified 9 variants, and identified three that had improved up to 13- and 340-fold for the toxic isomers of GD, up to 7-fold for GB, and up to 9-fold for GF, with respect to the starting point variant 2D8. Although their activities with GB ($1.7\text{-}3.2x10^6$ [M^{-1} min^{-1}]) were 3-6-fold lower than our desired goal, their catalytic efficiencies with GF and GD were well over $1x10^7$ [M^{-1} min^{-1}].

C. Catalytic activity of evolved variants with GA

The *in-vivo* toxicity of GA is >2-fold lower than that of all other G-agents[5], thus ranking its toxicity as the least threatening of the group. However, its structure (**Figure 1a**) is significantly different than that of all the other G-agents, and its R_P isomer is more toxic than its S_P isomer. Therefore, we decided to examine the ability of wild-type like rePON1, and of the most improved variants from each round of evolution, to hydrolyze GA. Using the AChE inhibition assay, we found that wt rePON1 (G3C9) is 3-30-fold more efficient at hydrolyzing the toxic isomer of GA than the toxic isomers of all other G-agents (**Table 7**). In addition, we found that our most improved variants from rounds 3 and 4, 1-I-F11 and IIG1, were 4-5 fold more efficient than rePON1 at hydrolyzing the toxic isomer of GA (**Table 7**). Thus, in spite of any direct selection pressure, the catalytic activity of our evolved variants with GA ($1.7\text{-}2.3$ $x10^6$ M^{-1} min^{-1}) had increased and had become similar to their activity on GB ($3.2\text{-}3.9$ $x10^6$ M^{-1} min^{-1}]).

D. Stereospecificity of the evolved variants

Our previous efforts to evolve PON1 for hydrolysis of G-agents made use of their coumarin analogues[1]. In these compounds, the fluoride leaving group is replaced by a coumarin derivative (**Figure 1b)**, thus permitting fluorogenic or colorimetric detection of enzymatic activity[26]. Due to its pKa value (3.1), fluoride is a better leaving group than 3-cyano-7-hydroxy-4-methylcoumarin (pKa = 6.51±0.04), and is also much smaller. Nevertheless, the activities of OP-hydrolyzing enzymes on the coumarin analogues and on the actual G-type nerve agents have been shown to be quite similar not only for engineered PON1 variants[1], but also for other OP-hydrolyzing enzymes, such as PTE[31]. In this project, the hydrolysis of G-agents was monitored making use of the AChE assay that detects only hydrolysis of their toxic S_P isomers. To examine the hydrolysis of both stereoisomers, we assayed the most improved variants from each round of directed evolution using the purified R_P and S_P isomers of the coumarin analogue of GF (CMP-coumarin; **Figure 1b**). The results indicate that the increase in detoxification rates for the three target G-

agents (GB, GD and GF) along the course of directed evolution was accompanied by a complete reversion in rePON1 stereoselectivity in favor of the S_P isomer (**Table 7**). The catalytic activity of the wild-type-like rePON1 on R_P-CMP-coumarin is >400-fold higher than on S_P-CMP-coumarin. In contrast, the catalytic activity of the best variants from round 3 and 4 on S_P-CMP-coumarin was found to be >4000-fold higher than their activity on R_P-CMP-coumarin **(Table 8**).

We were able to attribute the increase in S_P/R_P stereoselectivity with CMP-coumarin to changes both in substrate binding and catalysis. We observed a gradual decrease in K_m values for S_P-CMP-coumarin with each round of evolution together with a concomitant increase in k_{cat} values (**Table 8**). A parallel, gradual increase in K_m, aaccompanied by a decrease in k_{cat} values, was observed for the same variants with R_P-CMP-coumarin. The change in the enantiomeric ratio (E) differed from round to round, with the most dramatic change occurring in round 3 variants. A similar trend was observed when we examined the hydrolysis of the coumarin analogue of GD, PMP-coumarin. Unlike other G-agents, GD has a chiral carbon atom in addition to its chiral phosphorus center (**Figures 1a & 1b**). As with other G-agents, the toxicity of GD is determined by the phosphorus chirality, and GD's two S_P isomers (S_PR_C, S_PS_C) are >1000-fold stronger inhibitors of AChE than its two R_P isomers (R_PS_C, R_PR_C)[32]. While the best round 1 variant, PG11, hydrolyzed all four diasteroisomers of PMP-coumarin at measurable rates, variants from rounds 2-4 hydrolyzed only 50% of the racemic mixture. To confirm that the hydrolyzed fraction corresponds to the S_P isomer pair, we made use of the evolved rePON1 variant 3B3, that had previously been shown to hydrolyze almost exclusively the R_P isomers of various coumarin OPs, including *O*-ethyl methylphosphonyl-coumarin, *O*-n- or *O*-i-propyl methylphosphonyl-coumarin, and *O*-cyclohexyl methylphosphonyl-coumarin (CMP-coumarin)[33]. Here, we observed that 3B3 was able to hydrolyze only 50% of a racemic mixture of PMP-coumarin, and that the remaining 50% was readily hydrolyzed by evolved variants from rounds 2-4 (not shown). We thus conclude that in response to the continuous application of a screen for protection of AChE, which identifies enzymes that target the S_P isomers of the applied G-agents, our evolved variants became highly specialized for S_P isomer hydrolysis

E. Generation of PON1 variants specific for V-type nerve agents

The evolution of V-type hydrolyzing variants has lagged behind the development of G-type hydrolyzing variants primarily due to the lack of suitable V-agent surrogates. Variants that failed to hydrolyze the *O,O*-diethylphosphoryl analog of V-type nerve agents, amiton $(C_2H_5O)_2P(O)SCH_2CH_2N(Et)_2$ (Fig. 4), were subsequently found to exhibit low, yet detectable, activity on the *O*-alkyl methylphosphonothiolates (*e.g.*, VM, VX, RVX). Variants belonging to earlier generations (*e.g.*, wt-G3C9, 3B3, 1A4, 0C9, 2D8), hydrolyzed VM at 2-5 mU/mg compared to 40 mU/mg displayed by bacterial wt PTE. Amiton is hydrolyzed by PTE (50 mU/mg) but not by the rePON1 variants mentioned above. Thus, VM, rather than amiton, can serve as a suitable VX analog for identification of rePON1 variants capable of hydrolyzing P-S-alkyl containing nerve agents. In order to develop an efficient screening procedure for identification of variants capable of efficiently degrading V agents, we again utilized the enzymic approach with hAChE added to the lysates. For this purpose, we developed an *in situ* non-hazardous synthetic procedure for the generation of two pairs of methylphosphonothiolates that differ in the size of the *O*-alkyl moiety, namely VX and its homolog VM, and RVX and its homolog RVX-isoPr (**Fig. 4**). Our first (Round 1) VX library was made by screening lysates of the R4 G agent library (**Table 6b**) with VX, utilizing the ISA protocol based on inhibition of hAChE. We isolated and characterized 3 improved variants from that round, which displayed

>200-fold enhanced hydrolysis of VX relative to wt-rePON1 (**Table 9**). We then used VX to assay the catalytic efficiency of variants isolated and purified from all previous rounds of G-agent evolution. Although variants from earlier rounds of G-type evolution were less active on VX, they had different mutational compositions. We therefore combined the 4 variants from earlier rounds with the highest activity towards VX with the 3 most active R4 variants referred to above, which were denoted VX-R1, and shuffled them together to generate a Round 2 library of VX mutants (VX-R2 library).

The round 2 library was screened again against VX and RVX, and it was possible to isolate and characterize 4 variants that showed significantly improved VX hydrolysis. The best VXR2 variant was S-2-C8 (**Table 9**). In conclusion, efforts towards achieving this milestone have resulted, so far, in at least one variant capable of hydrolyzing the toxic isomer of VX >5000-, >130- and >25-fold better than the wt-G3C9, 4E9 and the VXG1 variants, respectively (**Table 9**). Thus, S-2-C8 hydrolyzed the toxic isomer of VX at $1.0x10^4$ M^{-1} min^{-1}, a value similar to that for a bacterial PTE that we had used to verify the interception protocol with V agents (**Table 9**). To gain further insight into the stereo-preference of S-2-C8 when reacting with the racemic VX, release of the leaving group, $HSCH_2CH_2N(isoPr)_2$, was monitored by use of Ellman's reagent, DTNB. Fig. 5 clearly shows that the two optical isomers of VX are hydrolyzed equally well by S-2-C8. A similar kinetic time course, albeit slower, was observed with VM (not shown). RVX and RVX-isPr were found, however, to be poor substrates, suggesting that although the binding pocket in this variant accommodates the *O*-ethyl moiety well, it needs to be enlarged to permit enhanced hydrolysis of the *O*-isobutyl-containing V agents.

To further improve the VX hydrolysis capacity of PON1 we screened a round 3 VX library VX (VXR3), which was made by shuffling the 10 best clones of round 2 with oligos introducing 34 new site-specific mutations. We identified 19 improved variants from ~1000 random clones. Then we purified and characterized 4 of them. The best variant, 1-1-H3, was improved by 3.5-fold over the best variant of the previous round, S-2-C8, and had k_{cat}/K_m ~35,000 [$M^{-1}min^{-1}$] towards the toxic isomer of VX. Notably, when the rate of release of the leaving group, $HSCH_2CH_2N(iPr)_2$, was determined using DTNB, k_{cat}/k_m for 1-1-H3 was slightly lower, ~$2.4x10^4$ $M^{-1}min^{-1}$, suggesting that the two isomers of VX are hydrolyzed at different, albeit low, rates. When detoxification of RVX was followed by the enzymic protocol, 1-1-H3 displayed poor activity, and could not be determined; however, hydrolysis of the second half, *i.e.*, of the less toxic isomer, as evaluated using DTNB, was ~700 M^{-1} min^{-1}. VM, the *N*,*N*,-diethyl analog of VX was hydrolyzed at approximately $1x10^4$ M-1min-1, thus indicating that the steric constraint presented by the isobutyl moiety of RVX does not permit proper accommodation in the catalytic site. Results from screening the VXR3 library were taken into consideration in building the VXR4 library.

We made three libraries of variants by shuffling the 10 best clones from round VXR3 and introducing mutations at 4 new positions. The three libraries differed in the number of new mutations introduced per variant: 1, 1.5 and 2.5 on average. Novel mutations were observed in 2 positions. The preliminary results from the enzymic protocol processed in well lysates show a ~10-fold increase in proficiency towards VX when compared to VXR3 library. The most active VXR4 variant displayed $k_{cat}/K_m=1.5x10^5$ $M^{-1}min^{-1}$, >75,000-fold greater than the wt G3C9 enzyme.

F. *Ex-vivo* experiments in human whole blood[2]

Ex vivo protocol: In order to evaluate the stability and proficiency of rePON1 variants in human blood we developed an *ex-vivo* protocol to screen the potential antidotal capacity of rePON1 variants via their protection of endogenous acetylcholinesterase (AChE) and butyrylcholinesterase (BChE) in human whole blood obtained from a local blood bank. This protocol permitted us to address the relationship between blood rePON1 concentrations, together with their kinetic parameters, and the level of protection conferred on the ChEs in human blood following a challenge with GF. The GF was generated *in situ* at a non-hazardous concentration. In addition, long-term incubation of the tested rePON1 variants with whole blood, prior to spiking with GF, provided information concerning the effect of their association with blood components on their stability. For example, *ex-vivo* treatment of human whole blood with 0.45 μM VIID2 (an R4 variant) resulted in retention of 42% of the total ChE activity following spiking with 0.08 μM GF, compared to only 5% in unprotected blood. These experimental data are in good agreement with the % residual activities calculated on the basis of the rate constants for inhibition of human AChE and BChE by GF, the concentration of the rePON1 variant, and its k_{cat}/K_m value. The validation protocol developed provides a rapid and reliable *ex-vivo* screening tool for selection of rePON1 bioscavenger candidates suitable for use in the protection of humans against OP intoxication. The results also provide input for a revised mathematical model for estimating the efficacious dose required in humans of a given rePON1 variant.

The use of evolved PON1 variants as prophylactic drugs requires that they maintain their catalytic activity in the complex chemical and biological environment of human blood over long periods of time. Previously, we showed that evolved variants 4E9 and VIID2 were able to protect human blood cholinesterases (ChE) from inhibition by GF using an *ex-vivo* assay[34]. Here we examined the duration of blood ChE protection from GF using representative variants from each round of selection. In order to do so, we added purified variants PG11, VIID11, 1-I-F11 and VIID2 (from rounds 1-4 respectively), to human blood samples, followed by incubation at 37°C for 24 h. Samples of blood-PON1 variant mixtures were then spiked with *in situ* generated GF at different time intervals, and their residual ChE activity was then measured. The ability of each variant to protect blood ChE from inhibition by GF at each time point was then calculated relative to its initial protection activity obtained after only 5 min of incubation in blood (**Figure 6, upper panel**). While round 1 variant PG11 could not provide measurable ChE protection at the PON concentration range used (0.5-2.1μM) due to its low catalytic activity, variants VIID11, 1-I-F11 and VIID2 were able to maintain 80±2 %, 95±12 % and 95±2 % of their initial ChE protection activity in human blood following 24 h incubation at 37°C. The ChE activity of blood samples not containing PON variants exhibited no detectable changes following 24 h of incubation at 37°C (data not shown).

We then examined the stability of our evolved variants under the same conditions by assaying their ability to hydrolyze a chromogenic analogue of GF, CMP-coumarin, at various time intervals (**Figure 6. Lower panel)**. This assay provides an assessment of the variants stability by directly reporting on their catalytic activity. Samples of blood-PON1 mixtures incubated at 37°C were diluted 1000-fold into buffered solutions containing CMP-coumarin, and the rate of substrate hydrolysis (*i.e.,* release of the coumarin leaving group) was monitored for 5 min at 400 nM. The results were plotted as percent of the initial activity at t = 0 (**Figure 6, lower panel**). As with the previous assay, variants VIID11, 1-I-F11 and VIID2 maintained: 77±12%,

[2] For experimental details see Ashani *et al* (2011) ref #34.

95±6 % and 92±5% of their initial activities following a 24 h incubation period in human blood samples (*ex-vivo*) at 37°C. The stability of variant PG11 (76±5 %) was similar to that of 1-I-F11. Surprisingly, the activity of all variants after 1 h incubation increased 4-12% relative to their activity after 5 min. The spontaneous hydrolysis of CMP-coumarin by blood samples devoid of any PON1 variant was found to be negligible (data not shown). The results from the *ex-vivo* experiments were similar to the stability of the 4 best variants observed in Tris buffer, pH 7.4 (37°C) (**not shown**). Thus, taken together, these results indicate that the *ex vivo* interaction of the evolved PON1 variants with human blood constituents did not affect their proficiency at least for 24 h at 37°C.

Key Research Accomplishments

- Development of a screen for PON1 variants with increased OP activity, based on sorting emulsion droplet by FACS.
- Development of a novel neutral drift PON1 library
- Synthesis of amiton, a P-S model compound for VX, and safe and non-hazardous procedures for *in situ* generation of G- and V-type nerve agents
- Protocol for stereo-specific synthesis of a chiral *O*-alkyl methylphosphonate with a coumarin fluorescent leaving group
- Interception protocol (ISA) for direct screening of crude lysates with G-type nerve agents
- Isolation, overexpression and purification of several variants with greatly enhanced hydrolysis towards GA, GB, GD. GF, (k_{cat}/K_m of 2-5x10^7 $M^{-1}min^{-1}$) and towards VX (k_{cat}/K_m=1.5x10^5 $M^{-1}min^{-1}$).
- Libraries of variants capable of hydrolyzing G- and V-type nerve agents
- 3D structures of wt rePON1 and of 5 additional catalytically active PON1 variants.
- A protocol for *ex-vivo* estimation of k_{cat}/K_m values of rePON1 variants in human blood
- Several variants were over-expressed, purified and transferred along with their plasmid to USAMRICD (Aberdeen Proving Ground, MD) and to the Department of Biochemistry, Ohio State University, for further *in vivo* evaluation of protection against G-type nerve agent intoxication (including variants: 2C3, 3D8, 8C8, 1G3, 3B3, 2H4, 0C9, 2D8 and 1A4, 4E9, MG2-1A4, VIID2).

Reportable Outcomes

a) Goldsmith M, Ashani Y, Simo Y, Ben-David M, Leader H, Silman I, Sussman JL, Tawfik DS. 2011. Evolved stereoselective hydrolases for broad-spectrum G-type nerve agent detoxification. *Chem Biol* (submitted).

b) Gupta RD, Goldsmith M, Ashani Y, Simo Y, Mullokandov G, Bar H, Ben-David M, Leader H, Margalit R, Silman I, Sussman JL, Tawfik DS. 2011. Directed evolution of hydrolases for prevention of G-type nerve agent intoxication. *Nat Chem Biol 7*:120-125 (attached).

c) Ashani Y, Goldsmith M, Leader H, Silman I, Sussman JL, Tawfik DS. 2011. *In vitro* detoxification of cyclosarin in human blood pre-incubated *ex vivo* with recombinant serum paraoxonases. *Toxicol Lett 206*:24-28.

d) Ashani, Y., Goldsmith, M., Gupta, R., Leader, H., Margalit, R., Ben-David, M., Silman, I., Sussman, J.L., Tawfik, D.S. The use of recombinant paraoxonases as bioscavengers for the pretreatment/treatment of organophosphate poisoning, 13th Medical Chemical Defense Conference, April 2011, Munich, Germany

e) Ashani, Y., Goldsmith, M., Leader, H., Ben-David, M., Silman, I., Sussman, J.L. Tawfik, D.S. Progress in evolution of catalytic bioscavengers for OP nerve agents: Towards a broad spectrum detoxifying variant, CBD S&T Conference, November 2011, Las Vegas, Nevada, USA

f) Ashani Y, Gupta RD, Goldsmith M, Silman I, Sussman JL, Tawfik DS, Leader H. 2010. Stereo-specific synthesis of analogs of nerve agents and their utilization for selection and characterization of Paraoxonase (PON1) catalytic scavengers. *Chem Biol Interactions 187*:362-369 (attached).

g) Dvir H, Silman I, Harel M, Rosenberry TL, Sussman JL. 2010. Acetylcholinesterase: From 3D structure to function *Chem Biol Interact 187*:10-22.

h) Sussman JL, Silman I. 2009. Structural studies on acetylcholinesterase and paraoxonase directed towards development of therapeutic biomolecules for the treatment of degenerative diseases and protection against chemical threat agents In: Sussman JL and Spadon P, eds. *From Molecules to Medicines Structure of Biological Macromolecules and Its Relevance in Combating New Diseases and Bioterrorism*. Dordrecht: Springer Netherlands. Vol. XV, pp 183-199.

i) Khersonsky O, Rosenblat M, Toker L, Yacobson S, Hugenmatter A, Silman I, Sussman JL, Aviram M, Tawfik DS. 2009. Directed evolution of serum paraoxonase PON3 by family shuffling and ancestor/consensus mutagenesis, and its biochemical characterization. *Biochemistry 48*:6644-6654.

j) Gaidukov L, Bar D, Yacobson S, Naftali E, Kaufman O, Tabakman R, Tawfik DS, Levy-Nissenbaum E. 2009. In vivo administration of BL-3050: highly stable engineered PON1-HDL complexes. *BMC Clin Pharmacol 9*:18.

k) Tokuriki N, Tawfik DS. 2009. Chaperonin overexpression promotes genetic variation and enzyme evolution. *Nature 459*:668-673.

l) Gupta RD, Tawfik DS. 2008. Directed enzyme evolution via small and effective neutral drift libraries. *Nat Methods 5*:939-942 (attached).

m) Ashani, Y., Ben-David, M., Devi-Gupta, R., Greenblatt, H.M., Leader, H., Mullokandov, G., Silman, I., Tawfik, D.S., and Sussman, J.L. 2008 Biochemical and Structural Analyses of Chiral Methylphosphonate Analogues of G- and V-agents for High-Throughput Screening of Reversed Stereoselectivity of Paraoxonase-1 Variants, Presentation at the 16th Biennial Medical Defense Bioscience Review, USAMRICD, June 1-6, Marriott Hotel, Hunt Valley MD

n) Colletier JP, Bourgeois D, Sanson B, Fournier D, Sussman JL, Silman I, Weik M. 2008. Shoot-and-Trap: use of specific x-ray damage to study structural protein dynamics by temperature-controlled cryo-crystallography. *PNAS 105*:11742-11747.

o) Xu Y, Colletier J-P, Weik M, Jiang H, Moult J, Silman I, Sussman JL. 2008. Flexibility of aromatic residues in the active-site gorge of acetylcholinesterase: X-ray versus molecular dynamics. *Biophys J 95*:2500-2511 (attached).

p) Xu Y, Colletier JP, Jiang H, Silman I, Sussman JL, Weik M. 2008. Induced-fit or pre-existing equilibrium dynamics? Lessons from protein crystallography and MD simulations on acetylcholinesterase. *Protein Sci 17*:601-605.

q) Peisajovich SG, Tawfik DS. 2007. Protein engineers turned evolutionists. *Nat Methods 4*:991-994.

r) Harel M, Brumshtein B, Meged R, Dvir H, Ravelli RBG, McCarthy A, Toker L, Silman I, Sussman JL. 2007. 3-D Structure of serum paraoxonase 1 sheds light on its activity, stability, solubility and crystallizability. *Arch Ind Hyg Toxicol 58*:347-353.

Conclusions

Directed evolution, combining random and designed mutations based on 3D structures, resulted in the identification, expression and purification of mutants of a recombinant mammalian PON1 (rePON1) with catalytic activity that approaches the theoretical estimated minimal requirement for efficient prophylactic protection at reasonable protein doses. The k_{cat}/K_m values for these variants, when reacting with G-type CWNAs, are as high as $2\text{-}5x10^7$ $M^{-1}min^{-1}$, and it is envisaged that this proficiency will be further increased by additional rounds of directed evolution, and thus further decrease the loading dose of the protecting enzyme. The most advanced mutants were evolved to completely reverse the stereo-preference of PON1 from the non-toxic to the toxic isomers of racemic nerve agents. PON1 variants evolved by selection with VX are capable of hydrolyzing the toxic isomer of VX >75,000-fold faster than the wt enzyme, with $k_{cat}/K_m=1.5x10^5$ $M^{-1}min^{-1}$. Additional rounds will be required to obtain the efficiency required to qualify PON1 as antidotes against VX ($k_{cat}/K_m >1x10^7$ $M^{-1}min^{-1}$). These results, taken together with preliminary *in vivo* evaluation (performed at ICD, Aberdeen Proving Ground MD), suggest that one or two PON1 variants might serve as broad-spectrum catalytic bioscavengers to protect against multiple LD50 doses of all realistic CWNA threat agents at low protein doses. This technology is further envisaged to provide rapid discovery of pretreatment and post-challenge therapeutic drugs not only against existing threats but also to counteract emerging OP-based CWNA and commercial pesticides, and thus shorten the time from emergence of a threat to identification of potential antidotes measures to a few days or weeks.

References

1. Gupta, R.D. *et al.* Directed evolution of hydrolases for prevention of G-type nerve agent intoxication. *Nat. Chem. Biol.* **7**, 120-125 (2011).
2. Aharoni, A. *et al.* Directed evolution of mammalian paraoxonases PON1 and PON3 for bacterial expression and catalytic specialization. *Proc. Natl. Acad. Sci. USA* **101**, 482-487 (2004).
3. Harel, M. *et al.* Structure and evolution of the serum paraoxonase family of detoxifying and anti-atherosclerotic enzymes. *Nat. Struct. Mol. Biol.* **11**, 412-419 (2004).
4. Romano, J.A., Lukey, B.J. & Salem, H. Chemical warfare agents: chemistry, pharmacology, toxicology, and therapeutics. Vol. XXV 723 (2008).
5. Benschop, H.P. & de Jong, L.P.A. Nerve agent stereoisomers: analysis, isolation, and toxicology. *Acc. Chem. Res.* **21**, 368-374 (1988).
6. Benschop, H.P., Konings, C.A.G., Van Genderen, J. & De Jong, L.P.A. Isolation, Antiocholinesterase Properties, and Acute Toxicity in Mice of the Four Stereoisomers of the Nerve Agent Soman. *Toxicol. Appl. Pharmacol.* **72**, 61-74 (1984).
7. Newmark, J. Nerve Agents. *Neurologist* **13**, 20-32 (2007).
8. Dunn, M.A. & Sidell, F.R. Progress in medical defense against nerve agents. *JAMA* **262**, 649-652 (1989).
9. Cannard, K. The acute treatment of nerve agent exposure. *J. Neurol. Sci.* **249**, 86-94 (2006).
10. Bird, S.B., Dawson, A. & Ollis, D. Enzymes and bioscavengers for prophylaxis and treatment of organophosphate poisoning. *Front. Biosci. (Schol Ed)* **2**, 209-220 (2010).
11. Lenz, D.E. *et al.* Stoichiometric and catalytic scavengers as protection against nerve agent toxicity: a mini review. *Toxicology* **233**, 31-39 (2007).
12. Doctor, B.P. & Saxena, A. Bioscavengers for the protection of humans against organophosphate toxicity. *Chem. Biol. Interact.* **157-158**, 167-171 (2005).
13. Theriot, C.M. & Grunden, A.M. Hydrolysis of organophosphorus compounds by microbial enzymes. *Appl. Microbiol. Biotechnol.* **89**, 35-43 (2011).
14. diTargiani, R.C., Chandrasekaran, L., Belinskaya, T. & Saxena, A. In search of a catalytic bioscavenger for the prophylaxis of nerve agent toxicity. *Chem. Biol. Interact.* **187**, 349-354 (2010).
15. Ashani, Y. & Pistinner, S. Estimation of the upper limit of human butyrylcholinesterase dose required for protection against organophosphates toxicity: a mathematically based toxicokinetic model. *Regulatory Toxicol. Pharmacol.* **77**, 358-367 (2004).
16. Khersonsky, O. & Tawfik, D.S. Structure-reactivity studies of serum paraoxonase PON1 suggest that its native activity is lactonase. *Biochemistry* **44**, 6371-6382 (2005).
17. Costa, L.G., Giordano, G. & Furlong, C.E. Pharmacological and dietary modulators of paraoxonase 1 (PON1) activity and expression: the hunt goes on. *Biochem. Pharmacol.* **81**, 337-344 (2011).
18. Mackness, B. *et al.* Human tissue distribution of paraoxonases 1 and 2 mRNA. *IUBMB life* **62**, 480-482 (2010).

19. Seo, D. & Goldschmidt-Clermont, P. The paraoxonase gene family and atherosclerosis. *Curr. Atheroscler. Rep.* **11**, 182-187 (2009).

20. Amitai, G. *et al.* Enhanced stereoselective hydrolysis of toxic organophosphates by directly evolved variants of mammalian serum paraoxonase. *FEBS J.* **273**, 1906-1919 (2006).

21. Gaidukov, L. *et al.* In vivo administration of BL-3050: highly stable engineered PON1-HDL complexes. *BMC Clin. Pharmacol.* **9**, 18 (2009).

22. Gupta, R.D. & Tawfik, D.S. Directed enzyme evolution via small and effective neutral drift libraries. *Nat. Methods* **5**, 939-942 (2008).

23. Aharoni, A., Amitai, G., Bernath, K., Magdassi, S. & Tawfik, D.S. High-throughput screening of enzyme libraries: thiolactonases evolved by fluorescence-activated sorting of single cells in emulsion compartments. *Chem. Biol.* **12**, 1281-1289 (2005).

24. Mastrobattista, E. *et al.* High-throughput screening of enzyme libraries: in vitro evolution of a beta-galactosidase by fluorescence-activated sorting of double emulsions. *Chem. Biol.* **12**, 1291-1300 (2005).

25. Herman, A. & Tawfik, D.S. Incorporating Synthetic Oligonucleotides via Gene Reassembly (ISOR): a versatile tool for generating targeted libraries. *PEDS* **20**, 219-226 (2007).

26. Amitai, G. *et al.* Asymmetric fluorogenic organophosphates for the development of active organophosphate hydrolases with reversed stereoselectivity. *Toxicology* **233**, 187-198 (2007).

27. Ben-David, M. *et al.* Catalytic versatility and redundancy in enzyme active-sites: The case of serum paraoxonase 1. (in preparation) (2011).

28. Alcolombri, U., Elias, M. & Tawfik, D.S. Directed evolution of sulfotransferases and paraoxonases by ancestral libraries. *J. Mol. Biol.* **411**, 837-853 (2011).

29. Field, S.F. & Matz, M.V. Retracing evolution of red fluorescence in GFP-like proteins from Faviina corals. *Mol. Biol. Evol.* **27**, 225-233 (2010).

30. Bridgham, J.T., Carroll, S.M. & Thornton, J.W. Evolution of hormone-receptor complexity by molecular exploitation. *Science* **312**, 97-101 (2006).

31. Tsai, P.C. *et al.* Stereoselective hydrolysis of organophosphate nerve agents by the bacterial phosphotriesterase. *Biochemistry* **49**, 7978-7987 (2010).

32. Benschop, H.P., Konings, C.A., Van Genderen, J. & De Jong, L.P. Isolation, anticholinesterase properties, and acute toxicity in mice of the four stereoisomers of the nerve agent soman. *Toxicol. Appl. Pharmacol.* **72**, 61-74 (1984).

33. Ashani, Y. *et al.* Stereo-specific synthesis of analogs of nerve agents and their utilization for selection and characterization of Paraoxonase (PON1) catalytic scavengers. *Chem. Biol. Interact.* **187**, 362-369 (2010).

34. Ashani, Y. *et al. In vitro* detoxification of cyclosarin in human blood pre-incubated ex vivo with recombinant serum paraoxonases. *Toxicol. Lett.* **206**, 24-28 (2011).

Tables

Table 1. Activity of PON1 mutants with both isomers of CMP-coumarin and with S_P -IMP-coumarin

Variants	S_P-CMP coumarin [a] (k_{cat}/K_m) $M^{-1}min^{-1}$	S_P-IMP coumarin [a] (k_{cat}/K_m) $M^{-1}min^{-1}$	R_P-CMP coumarin [a] $\times 10^6$ Apparent (k_{cat}/K_m) $M^{-1}min^{-1}$	Non-synonymous mutations[c]
Wild-type-like rePON1-G3C9	<200 (1)[b]	n.d.	0.08±0.0034 (1)	-
H115W	331±39 (>1.6)	1983±30 (1)	0.45 (6) ↑	**H115W**
V346A	885±76 (>4.4) ↑	3633±126 (1.8)↑	0.2 (2.5) ↑	**V346A**
H115W+V346A	813±79 (>4.1) ↑	10140±7 (5) ↑	0.4 (5) ↑	**H115W**, **V346A**

a. For each variant, enzymatic activities (k_{cat}/K_m) were measured with purified proteins and denoted are the average ± standard deviation values obtained from 3 independent repeats. The values without standard deviations had s.d.≤20% of their values. Values in parentheses denoted the fold increase and decrease as compared to wt-like rePON1 for either isomer of CMP and as compared to H115W for S_P-IMP. n.d. denotes non-detectable activity.

b. The catalytic efficiency was estimated as described in Ref#1

c. Denoted in bold are mutations in active-site residues.

Table 2: Representative variants along the directed evolution process

Variant [a]	Mutations [b]	S_P-CMP-Coumarin [c]			R_P-CMP-Coumarin Apparent k_{cat}/K_M [c]	S_P-CMP-F Apparent k_{cat}/K_M [c]
		k_{cat} (min^{-1})	K_M (μM)	k_{cat}/K_M ($\mu M^{-1}min^{-1}$)	($\mu M^{-1}min^{-1}$)	($\mu M^{-1}min^{-1}$)
rePON1G3C9	(Wild-type-like)	nd	nd	<0.0002 (1)[d]	0.08±0.0034 (1)	0.13±0.03 (1)
3B3	N41D, S110P, **L240S,** H243R, F264L, N324D, **T332A**	nd	nd	<0.0002 (1) [d]	20±1.7 (250) ↑	~0.0001
H115W-V346A	**H115W, V346A**	nd	nd	0.0008 (>4) ↑	0.4 (5) ↑	0.02 ±0.003
3A7	V97A, **H115W**, P135A, **F222S**, M289I	nd	nd	0.0027 (>13.5) ↑	0.16 (2) ↑	0.008 ±0.0035
8C8	**L69S**, V97A, **H115W**, P135A, **F222S**	11.6 ±0.18	124.5 ±5.8	0.093 ±0.003 (>465) ↑	0.0035 (23) ↓	0.2 (1.5)
2D8	**L69G**, **H115W**, **H134R**, **F222S**, **T332S**	268 ±1.6	76.3 ±3.2	3.52 ±0.13 (>17600) ↑	0.465 (5.8) ↑	14.3 (110)
3D8	**L69G**, **H115W**, **H134R**, M196V **F222S**, **T332S**	295 ±1.62	25.4 ±0.5	11.6 ±0.23 (>58000) ↑	nd [e]	3.3 (25)
4E9	**L69G**, S111T, **H115W**, **H134R**, **F222S**, **T332S**	513	23	22.3 (>111500) ↑	nd [e]	16.8 (129)

a. Annotation of variants: The first digit relates to the plate number, and the following letter-digit to its location within the plate. For example, variant 3A7 = plate #3, well A7; n.d., not detectable.
b. Denoted in bold are mutations in active-site residues.
c. Enzymatic parameters were measured with purified proteins and comprise the average obtained from the 3 independent repeats. Error ranges represent the standard deviations observed between measurements. Values in parentheses describe the fold-change compare to the starting point, rePON-G3C9. The kinetic parameters for S_P-CMP-coumarin were spectrophotometrically measured with pure substrate samples. Parameters for R_P-CMP-coumarin were determined with the racemate, and for CMP-F with the *in situ* prepared substrate and an AChE inhibition assay.
d. The catalytic efficiency was estimated as described in Ref.[1].

Table 3. Improved 3rd round variants from libraries derived from rePON1-H115W-V346A.

Variants [a]	Fold improvement with S_P-IMP-coumarin [b]	Fold improvement with S_P-CMP-coumarin [b]	Non-Synonymous mutations [c]
4D2	0.3x	10x	L69S, H115W, P135A, F222S
8C8	0.4x	13x	L69S, V97A, H115W, P135A, F222S
6C5	2x	3x	V97A, H115W, P135A, F222S, M196V, M289I
1A8	1.3x	1.5x	L4P, V97A, H115W, P135A, F222S, M196V
1E3	0.2x	1.4x	A6T, V97A, H115W, P135A, F222S, D212N, M289I
7G10	0.5x	1.3x	L10S, H115W, F222S, M289I, V346A
8H4	0.7x	0.8x	V97A, H115W, P135A, F222S
8H3	0.8x	0.8x	V97A, H115W, P135A, F222S, I237V, L262F
1G1	1.2x	1.2x	V97A, H115W, F222S, M289I

a. **The annotation of the variants:** The first letter relates to the plate number, and the letter-digit to the location of the clone within this plate. For example, variant 4D2= plate # 4, well D2.
b. Shown are all variants that exhibited higher S_P -IMP-coumarin and S_P-CMP-coumarin activities in crude lysates relative to the H115W + V346A PON1 mutant. For each variant, enzymatic activities were measured in crude lysates, and denoted are the average values of fold improvement obtained from 3 independent repeats. The values had s.d.≤20% of their value.
c. Non-synonymous mutations observed in each variant. Mutations in active-site residues are noted in red.

Table 4. Improved variants from shuffling of the targeted substitutions library (6th round variants)).

	CMP(S_P)[b]			CMP[b] (R_P)	CMP[b] (racemic)	IMP[b] (S_P)	EMP[b] (S_P)	EMP[b] (S_P)	
Variant [a]	k_{cat} min^{-1}	K_m μM	k_{cat}/K_m $\mu M^{-1}min^{-1}$	k_{cat}/K_m $\mu M^{-1}min^{-1}$					**Non-synonymous mutations [c]**
8C8	11.6 ±0.18	124.5 ±5.8	0.093 ±0.003 (1)	0.0035 (1)	0.03(1)	0.022 (1)	0.08 (1)	0.2 (1)	**L69S**, V97A, **H115W**, P135A, **F222S**
2C3	149.5 ±0.87	212.7 ±5.5	0.7 ±0.01 (7.5) ↑	0.088 (25) ↑	0.62 (21) ↑	0.079 (3.6) ↑	0.88 (11) ↑	0.16 (1)	**L69G**, **H115W**, **H134R**, **F222S**, K233E
5H5	126 ±2	102 ±3.8	1.25 ±0.05 (13.4) ↑	0.2088(60) ↑	2.43 (81) ↑	0.76 (35) ↑	3.8 (48) ↑	0.8 (4) ↑	L10S, F28Y, **L69G**, **H115W**, **H134R**, **F222S**, **T332S**
0C9	185 ±2.5	65 ±3.6	2.85 ±0.1 (31) ↑	0.296 (85) ↑	3.56 (119) ↑	1.04 (47) ↑	6.67 (83) ↑	2.6 (13) ↑	L14M, **L69G**, S111T, **H115W**, **H134R**, **F222S**, **T332S**
2D8	268 ±1.6	76.3 ±3.2	3.52 ±0.13 (38) ↑	0.465 (133) ↑	3.04 (101) ↑	0.85 (39) ↑	6.8 (85) ↑	0.98 (5) ↑	**L69G**, **H115W**, **H134R**, **F222S**, **T332S**
1A4	185 ±1.5	51 ±1.7	3.63 ±0.1 (39) ↑	0.39 (111)↑	3.11 (104) ↑	0.85 (39) ↑	7.15 (89) ↑	2.2 (11) ↑	A6E, **L69G**, **H115W**, **H134R**, **F222S**, K233E, **T332S**, T326S
3D8	295 ±1.62	25.4 ±0.5	11.6 ±0.23 (125) ↑	nd [d]	4.73 (158)↑	4.6 (209) ↑	12 (150) ↑	6.2 (31) ↑	**L69G**, **H115W**, **H134R**, M196V, **F222S**, **T332S**

a. The annotation of variants: The first letter relates to the plate number, and the letter-digit to the location of the clone within this plate. For example, variant 3B3 = plate # 3, well B3.
b. For each variant, enzymatic activities (k_{cat}/K_m) were measured with purified proteins, and denoted are the average ± standard deviation values obtained from the 3 independent repeats. The individual values exhibited s.d.≤20%. Values in parentheses denoted the fold increase and decrease **as compare to 8C8**, the best variant of the previous round.
c. Denoted in bold are mutations in active-site residues.
d. Variant exhibited single-phase kinetics of product release when reacted with racemic CMP-coumarin, suggesting that the rates of hydrolysis for R_P- and S_P-coumarin are similar.

Table 5: Activities of selected rePON1 variants on S_P-CMP-coumarin and its fluoridated product CMP-F (cyclosarin).[a,b,c,d]

mutant	(S_P)CMP-coumarin	CMP-fluoridate	fluoridate/coumarin
8C8	0.09	0.2	2.2
3D8	11.6	3.3	0.3
0C9	2.8	11.1	3.9
2D8	3.5	14.3	4.1
1A4	3.6	11.3	3.1
2C3	0.7	0.47	0.7

a. The figures shown are values of $k_{cat}/K_M x10^6$ ($M^{-1}min^{-1}$)
b. Data for OP-coumarin are based on release of the chromophore monitored at 400 nm.
c. The k_{cat}/K_m values for the fluoridates were determined by monitoring the rate of loss of anti-AChE potency of the *in situ*-generated compound, assuming K_m>>[P-F]. Calculations are based on a single enzyme concentration selected to fit the dynamic range for determination of the apparent k_{obs} of loss of anti-AChE potency.
d. The coumarin leaving group was replaced by fluoride in racemic CMP-coumarin to yield the racemic fluoridate of CMP (CMP-F). It should be noted that the data for the hydrolysis of CMP-F can be attributed mostly to its toxic (S_P) isomer.

Table 6a. Sequences and fold improvement of selected variants from round 1.

A. Sequences and fold improvement with sarin.

			3.9	3.5	3.5	2	1.7	1.6	1.4	1.4	1.3	1.2	1.0	1.0	0.9	0.8	0
rePON1	Amino Acid	2D8	9C3	4F3	5B2	PIH12	PD4	PG3	PA2	IG6	3D6	IB3	5H8	9H3	JD4	PG11	E2B
69	L	G	V	V	V	L	V	V	V	V	V	V	V	V	V	V	V
70	K	K	K	K	K	N	K	K	Q	K	K	Q	K	K	K	K	K
71	Y	Y	Y	F	F	Y	I	I	Y	I	Y	Y	Y	I	Y	Y	Y
82	S	S	S	S	S	S	S	S	S	S	S	S	S	S	S	S	P
115	H	W	W	L	L	L	V	V	L	V	L	L	V	W	L	A	C
134	H	R	R	R	R	R	R	R	N	R	R	N	R	R	N	R	R
196	M	M	M	F	M	M	M	M	M	M	M	M	M	M	L	M	M
222	F	S	S	S	S	S	S	S	S	S	S	S	S	S	S	S	S
240	L	L	L	L	L	L	I	I	L	I	L	L	L	L	L	L	V
292	F	F	F	F	F	F	F	F	F	F	L	F	F	F	F	F	F
332	T	S	S	S	S	S	S	S	S	S	S	S	S	S	S	S	S

* First row – Fold Improvement in activity of each variant relative to control variant 2D8 as measured in cleared cell lysates. Numbers represent an average of 2 measurements with S.D. <10% of value.

** Second row – variant names.

B. Sequences and fold improvement with soman.

			5.2	4.9	3.7	3.3	3.0	2.5	2.5	2.5	2.5	2.4	2.4	2.3	2.3	2.2	2.2	1.7	1.4	1.2	1.0
rePON1	Amino Acid	2D8	PIH12	PG11	5H8	PG3	IG6	PD4	E2B	3D6	4G8	4F3	PA2	5B2	6C8	2D1	PF4	IB3	5A9	JD4	7A6
69	L	G	L	V	V	V	V	V	V	V	V	V	V	V	V	V	V	V	V	V	L
70	K	K	N	K	K	K	K	K	K	K	K	K	Q	K	S	K	K	Q	K	K	A
71	Y	Y	Y	Y	Y	I	I	I	Y	Y	Y	F	Y	F	Y	Y	Y	Y	D	Y	Y
82	S	S	S	S	S	S	S	S	P	S	S	S	S	S	S	S	P	S	S	S	S
115	H	W	L	A	V	V	V	V	C	L	V	L	L	L	V	A	C	L	V	L	C
134	H	R	R	R	R	R	R	R	R	R	R	R	N	R	R	R	R	N	R	N	R
196	M	M	M	M	M	M	M	M	M	M	L	F	M	M	M	M	M	M	M	L	M
222	F	S	S	S	S	S	S	S	S	S	S	S	S	S	S	S	S	S	S	S	S
227	L	L	L	L	L	L	L	L	L	L	L	L	L	L	L	L	L	L	S	L	L
240	L	L	L	L	L	I	I	I	V	L	L	L	L	L	L	V	V	L	L	L	L
292	F	F	F	F	F	F	F	F	F	L	F	F	F	F	F	F	F	F	F	F	F
309	D	D	D	D	D	D	D	D	D	D	G	D	D	D	D	D	D	D	D	D	D
332	T	S	S	S	S	S	S	S	S	S	S	S	S	S	S	S	S	S	S	S	S

* First row – Fold Improvement in activity of each variant relative to control variant 2D8 as measured in cleared cell lysates. Numbers represent an average of 2 measurements with S.D. <10% of value.

** Second row – variant names.

Table 6b: Catalytic activities of improved variants from each round of evolution

Variant	Mutations relative to rePON1 [a]	Round	Catalytic efficiency [b,d] (k_{cat}/K_M) x10^7 $M^{-1}min^{-1}$			
			GD[c] Fast	GD[c] Slow	GF	GB
rePON1	-	-	0.0055 ±0.0017	0.0015 ±0.0006	0.013[e] ±0.003	0.008 ±0.001
8C8	Leu69Ser, Val97Ala, His115Trp, Pro135Ala, Phe222Ser	*0*	0.0028 ±0.0006[f] (0.5)	0.0014 ±0.0004[f] (0.9)	0.015[e] ±0.005 (1.2)	0.0034 ±0.001 (0.4)
0C9	Leu14Met, Leu69Gly, Ser111Thr, His115Trp, His134Arg, Phe222Ser, Thr332Ser	*0*	0.34 ±0.03[f] (62)	0.026 ±0.0006[f] (17)	1.11[e] ±0.3 (85)	0.028 ±0.009 (4)
1A4	Ala6Glu, Leu69Gly, His115Trp, His134Arg, Phe222Ser, Lys233Glu, Thr326Ser, Thr332Ser	*0*	0.41 ±0.07[f] (75)	0.033 ±0.004[f] (22)	1.13[e] ±0.3 (87)	0.023 ±0.003 (3)
4E9	Leu69Gly, Ser111Thr, His115Trp, His134Arg, Phe222Ser, Thr332Ser	0	0.74 ±0.3 (135)	0.056 ±0.01 (37)	1.75[e] ±0.3 (135)	0.033 ±0.004 (4)
5H8	**Leu69Val, His115Val,** His134Arg, Phe222Ser, Thr332Ser	*1*	0.57 ±0.04 (104)	0.064 ±0.03 (43)	0.244 ±0.012 (19)	0.01 ±0.008 (1)
VI-D2	Leu69Val, His115Val, His134Arg, **Phe222Val,** Thr332Ser	*2*	1.4 ±0.2 (255)	0.33 ±0.2 (220)	0.28 ±0.017 (22)	0.023 ±0.001[f] (3)
MG2-I-A4	Leu69Val, His115Ala, His134Arg, **Phe222Met,** Thr332Ser	*2*	1.95 ±0.4 (355)	1.3 ±0.2 (867)	1.28 ±0.1 (98)	0.13 ±0.006 (16)
IV-D11	Leu69Val, His115Ala, His134Arg, **Met196Leu, Phe222Met,** Thr332Ser	*2*	2.5 ±0.2 (455)	0.73 ±0.3 (487)	1.06 ±0.08 (82)	0.12 ±0.012 (16)

II-A1	Leu69Val, **His115Leu,** His134Arg, **Phe222Met,** Thr332Ser	*2*	2.5 ±0.21 (455)	0.73 ±0.5 (487)	0.59 ±0.1 (45)	0.07 ±0.003[f] (9)
V-B3	Leu69Val, His115Val, His134Arg, **Phe222Met,** Thr332Ser	*2*	2.6 ±0.1 (473)	0.68 ±0.5 (453)	1.2 ±0.5 (92)	0.05 ±0.003[f] (6)
2-II-D12	**Lys70Asn,** His115Leu, His134Arg, Phe222Met, Thr322Ser	*3*	0.27 ±0.014 (49)	0.27 ±0.014 (180)	0.96 ±0.15 (74)	0.18 ±0.028 (23)
1-I-D10	**Leu55Ile,** Leu69Val, His115Ala, His134Arg, Phe222Met, **Ile291Phe,** Thr322Ser	*3*	0.87 ±0.076 (158)	0.87 ±0.076 (580)	2.11 ±0.33 (162)	0.31 ±0.063 (39)
I-IV-H9	**Leu55Ile,** Leu69Val, His115Leu, His134Arg, **Asp136His,** Phe222Met, **Ile291Leu,** Thr322Ser	*3*	4.2 ±0.5 (764)	4.2 ±0.5 (2800)	2.38 ±0.18 (183)	0.31 ±0.03 (39)
VH3	Leu69Val, His115Ala, His134Arg, Phe222Met, Ile291Leu, Thr332Ser	4	2.6 ±0.2 (473)	2.6 ±0.2 (1733)	2.8 ±0.2 (215)	0.3 ±0.11 (38)
VIID2	Leu55Ile, Leu69Val, His115Ala, His134Arg, His197Arg, Phe222Met, Ile291Leu, Thr332Ser	4	3.7 ±1 (673)	3.7 ±1 (2467)	3.9 ±1 (300)	0.17 ±0.014 (21)

a. Mutations relative to the wild-type like rePON1 variant G3C9[3]. Mutations that were newly introduced in a given round are denoted in bold.
b. Fold improvement relative to wt-like rePON1. Errors of values were derived from at least two independent measurements. The maximal deviation between different enzyme preparations was ≤2 fold (measured for VIID2).
c. Fast and slow hydrolysis of the two equally toxic isomers of GD (S_CS_P and R_CS_P).
d. Kinetic parameters were determined with the *in situ* generated G-agent and by assaying residual AChE activity. They thus relate to the toxic S_P isomer.
e. Values from ref[1]
f. Standard deviation

Table 7: Catalytic activities of the best variant from each round

Variant	Genotype[a]	Round	GD[b,c] k_{cat}/K_m x10^7 [$M^{-1}min^{-1}$] Fast	GD[b,c] k_{cat}/K_m x10^7 [$M^{-1}min^{-1}$] Slow	GF[b] k_{cat}/K_m x10^7 [$M^{-1}min^{-1}$]	GB[b] k_{cat}/K_m x10^7 [$M^{-1}min^{-1}$]	GA[b] k_{cat}/K_m x10^7 [$M^{-1}min^{-1}$]
rePON1	-	-	0.0055 ±0.002	0.0015 ±0.0006	0.013[d] ±0.003	0.008 ±0.001	0.043 ±0.007
2D8	Leu69Gly, His115Trp, His134Arg, Phe222Ser, Thr332Ser	*0*	0.4 ±0.1	0.015 ±0.003	0.46[d] ±0.01	0.025 ±0.002	0.082 ±0.005
Fold improvement relative to (rePON1)[e]			(73)	(10)	(35)	(3)	(2)
PG11	**Leu69Val, His115Ala**, His134Arg, Phe222Ser, Thr332Ser	*1*	1.43 ±0.3	0.32 ±0.04	0.2 ±0.03	0.02 ±0.005	0.006 ±0.001
Fold improvement R1 relative to variant 2D8 (rePON1)[e]			4 (260)	21 (213)	0.4 (15)	0.8 (3)	0.07 (0.1)
VII-D11	Leu69Val, His115Ala, His134Arg, **Phe222Met, Asp309Gly,** Thr332Ser	*2*	2.9 ±0.9	2.9 ±0.1	1.07 ±0.08	0.12 ±0.01	0.025 ±0.003
Fold improvement R2 relative to variant 2D8 (rePON1)[e]			7 (527)	193 (1933)	2 (82)	5 (15)	0.3 (0.6)
1-I-F11	**Leu55Met,** Leu69Val, His115Ala, His134Arg, Phe222Met, **Ile291Leu,** Thr322Ser	*3*	4.4 ±0.6	4.4 ±0.6	1.52 ±0.1	0.39 ±0.04	0.17 ±0.04

Fold improvement R3 relative to variant 2D8 (rePON1)[e]			11 (800)	293 (2933)	3 (117)	16 (49)	2 (4)
IIG1	Leu55Ile, Leu69Val, His115Ala, His134Arg, **Asp136Gln,** Phe222Met, Ile291Leu, Thr332Ser	*4*	5.1 ±0.6	5.1 ±0.6	3.4 ±0.3	0.32 ±0.01	0.23 ±0.004
Fold improvement R4 relative to variant 2D8 (rePON1)[e]			13 (927)	340 (3400)	7 (262)	13 (40)	3 (5)

g. Mutations relative to the wild-type like rePON1 variant G3C9[3]. Newly introduced mutations are denoted in Bold.
h. Kinetic parameters relate to the toxic S_P isomers of GB, GD and GF or to the toxic R_P isomer of GA.
i. Fast and slow hydrolysis of the two equally toxic isomers of GD ($S_C S_P$ and R_C S_P).
j. Values previously measured in[1]
k. Fold improvement in catalytic activity of the best variant of the denoted round relative to the starting variant 2D8, or to wild-type-like rePON1. R1-round 1, R2-round 2, R3-round 3, R4-round 4.

Table 8: Table 3. Stereoselectivity with S_P- and R_P-CMP-coumarin.

Round #	Variant	S_P-CMP-coumarin			R_P-CMP-coumarin			Ratio of S_P/R_P[c]
		k_{cat} (min^{-1})	K_M (μM)	k_{cat}/K_M ($\mu M^{-1}min^{-1}$)	k_{cat} (min^{-1})	K_M (μM)	k_{cat}/K_M ($\mu M^{-1}min^{-1}$)	
-	rePON1 (G3C9)[a]	n.d.[b]	n.d.[b]	<0.0002	4.5 (±0.05)	54 (±2.6)	0.08	<0.0025
1	PG11	632 (±5)	104 (±12)	6.1	88 (±2.5)	381 (±27)	0.231	26
2	VIID11	500 (±19)	105 (±1)	4.8	73 (±4)	999 (±98)	0.073	66
3	1-I-F11	1004 (±98)	83 (±4)	12.1	n.d.[b]	n.d.[b]	0.003	4033
4	VIID2	1188 (±24)	79 (±2)	15	13.8 (±1.3)	1664 (±222)	0.008	1875

a. Previously measured in[1]
b. n.d. - not detectable.
c. Ratio of catalytic activity (k_{cat}/K_M) on S_P-CMP-coumarin to the catalytic activity (k_{cat}/K_M) on R_P-CMP-coumarin.

Table 9: Progress in evolution of VX-hydrolyzing variants

Catalytic Activity (k_{cat}/K_m, $M^{-1}min^{-1}$) of PON1 Variants hydrolyzing the toxic isomers of V-type agents (inhibition of hAChE)

Variant	Round	VX	RVX
Wt-G3C9		<2	<2
8C8	VX-G0	93	
4E9	**VX-G0**	**80**	
VIIH3	VX-R1	413	327
VA4	VX-R1	487	249
IA12	VX-R1	288	114
S-2-C8	**VX-R2**	**10,600**	<200

NOTE: Bacterial PTE hydrolyzed VX at 8,500 $M^{-1}min^{-1}$

Figures

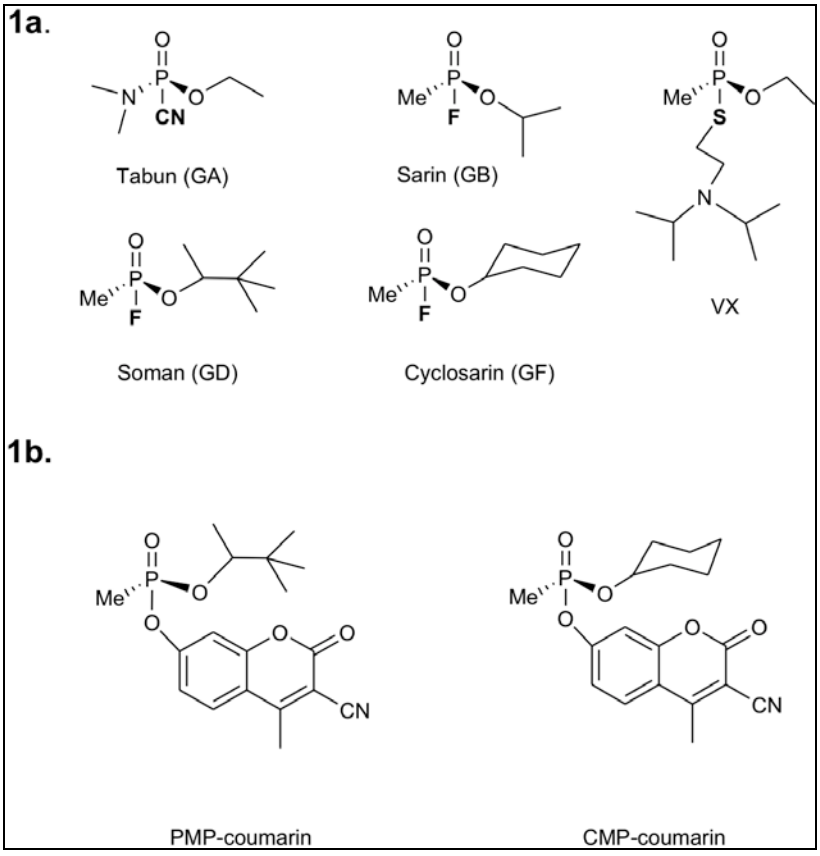

Figure 1. Nerve agents

(1a) G- and V-type type nerve agents: tabun (GA), sarin (GB), soman (GD), cyclosarin (GF) and VX

(1b) Coumarin analogs

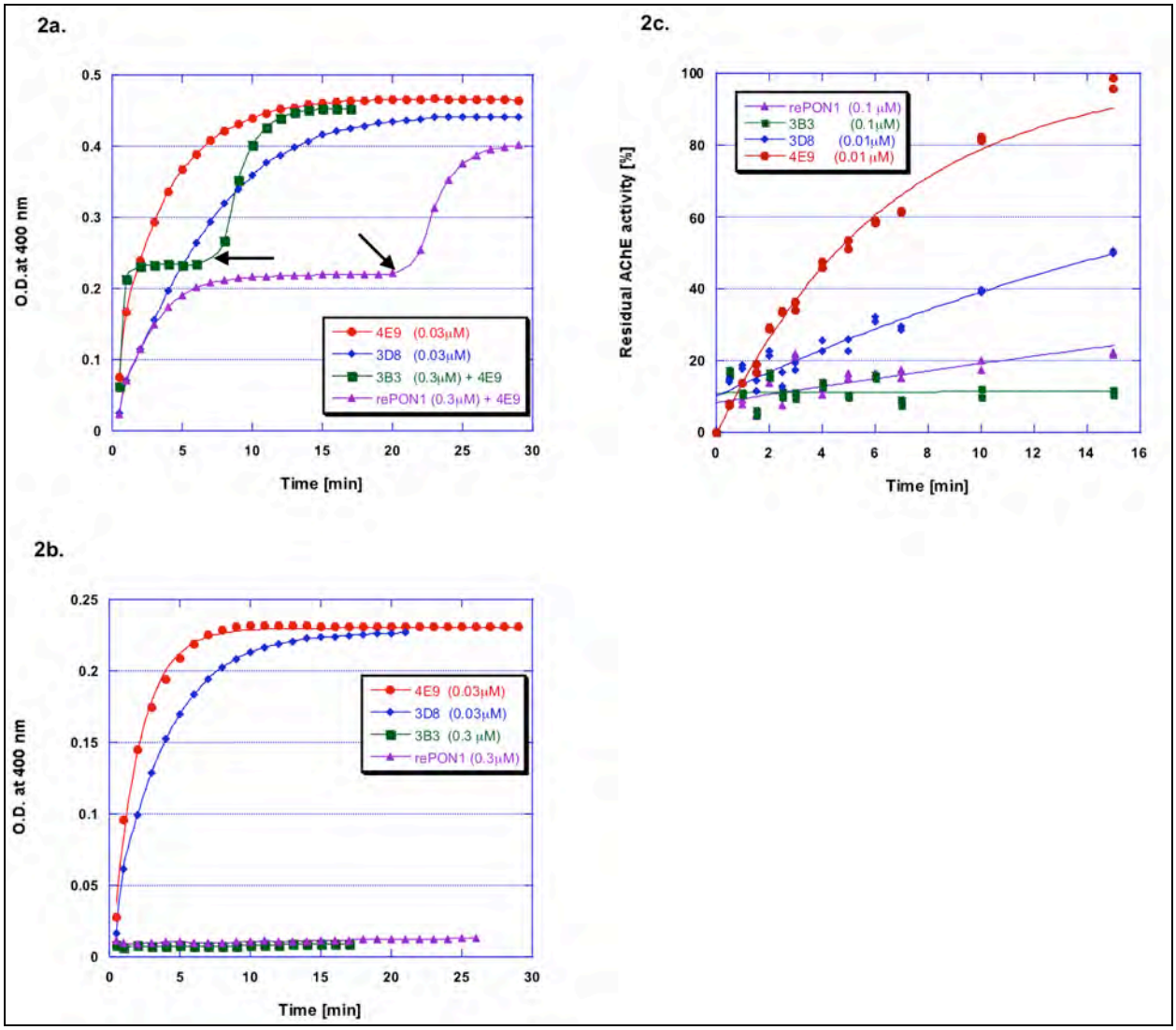

Figure 2. Hydrolysis of CMP-coumarin and CMP-F by rePON1 variants

Enzyme concentrations were varied depending on the variant's activity and are noted in the figure. (a) Hydrolysis of racemic CMP-coumarin (12 μM) in the presence of variants 4E9, 3D8, 3B3 (plus addition of 0.03 μM 4E9 after 6 min, indicated by the black arrow) and wt-like rePON1 (plus addition of 0.03 μM 4E9 after 20 min); (b) Hydrolysis of S_P-CMP-coumarin (6 μM) in the presence of variants 4E9, 3D8, 3B3 and rePON1; (c) Residual AChE activity was assayed after the incubation of *in situ*–generated CMP-F (40 nM) and 4E9, 3D8, 3B3 and rePON1 at the concentrations noted in the figure (data were fitted to a first-order rate equation to derive the apparent rate constant for hydrolysis of CMP-F; error bars represent the s.d. of two or more independent measurements)

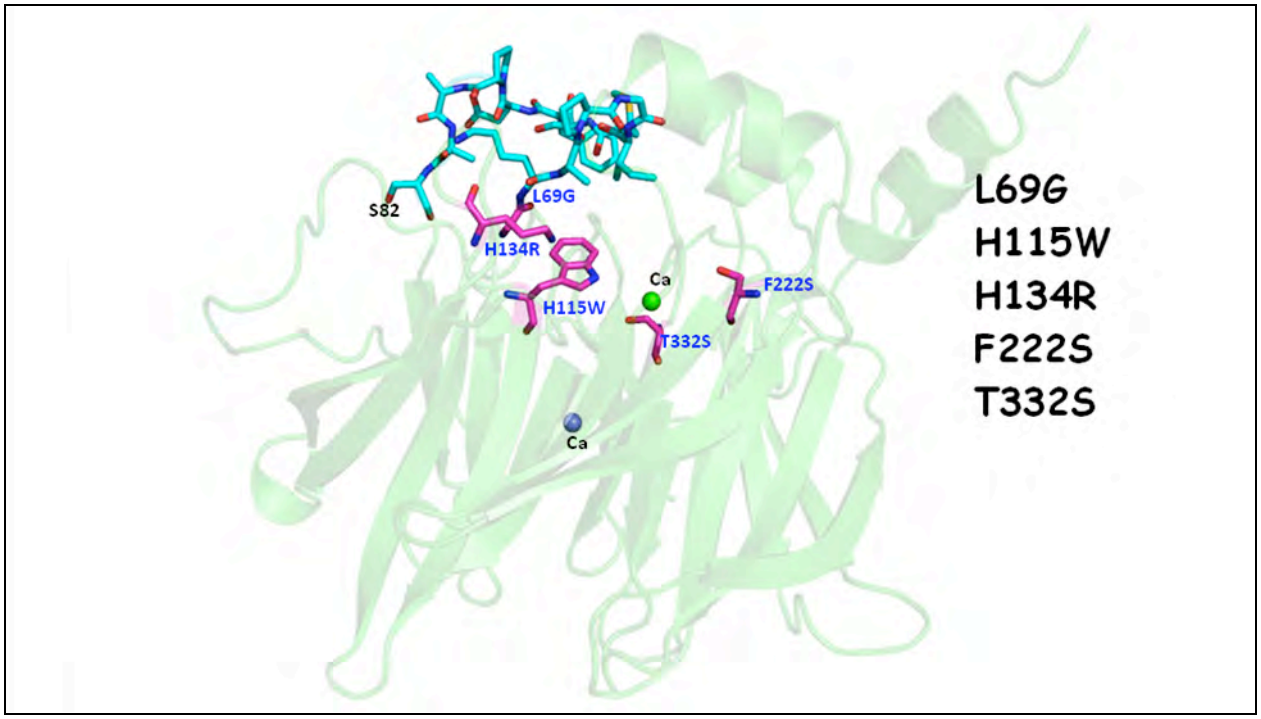

Figure 3. G2E6-PON1 penta-mutant (2D8) at 2.6 Å resolution (library of round 0). The flexible loop (cyan) covers the active site.

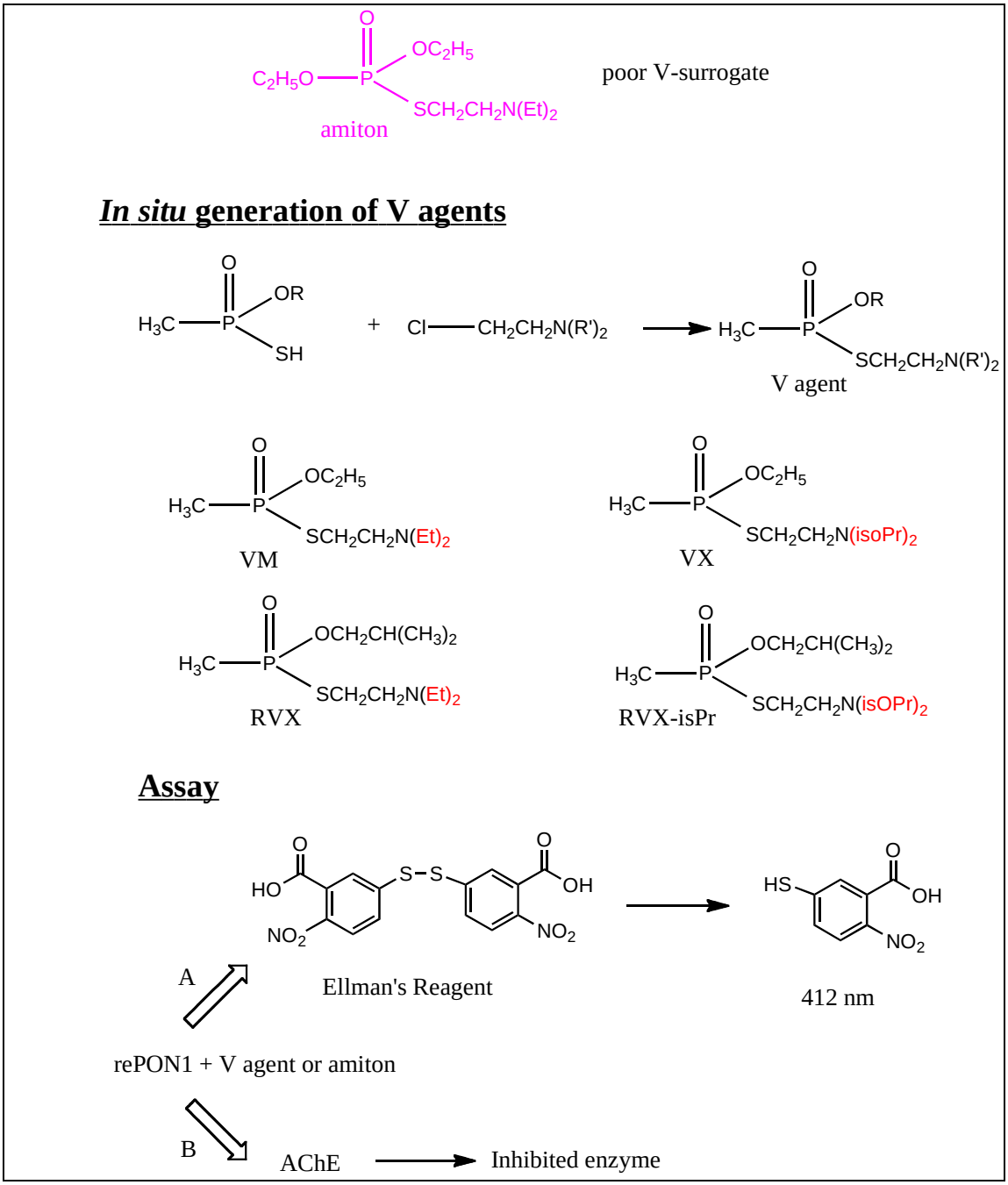

Figure 4. Synthesis and structures of V-type nerve agents.

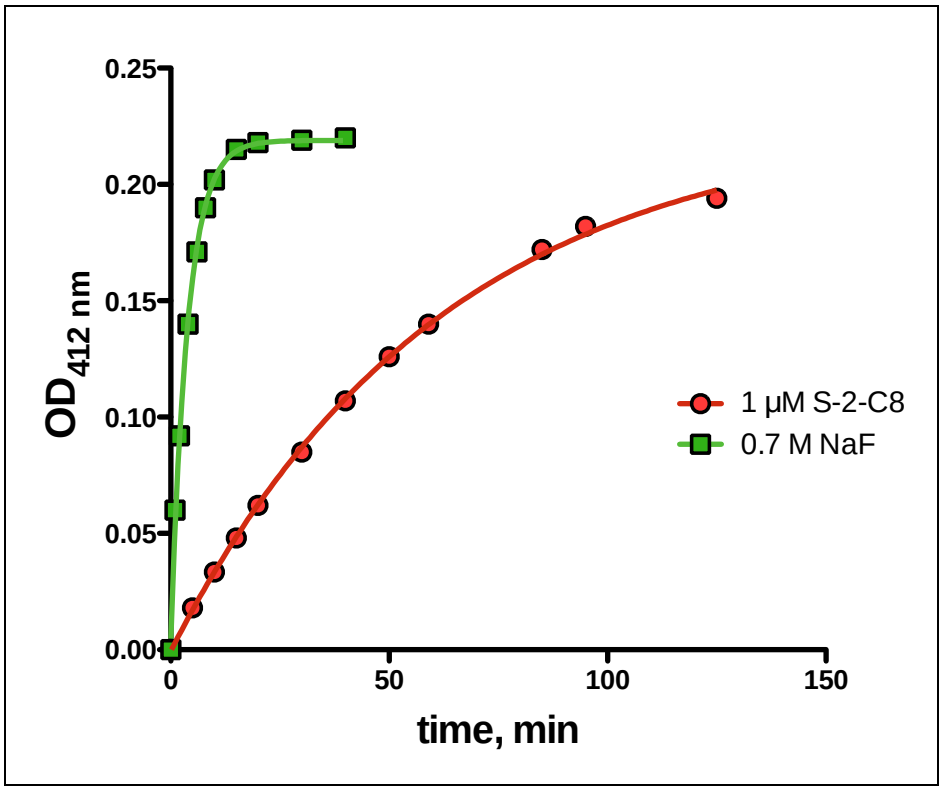

Figure 5. S-2-C8-induced hydrolysis of $1.7x10^{-5}$ M VX using DTNB to capture the leaving group.

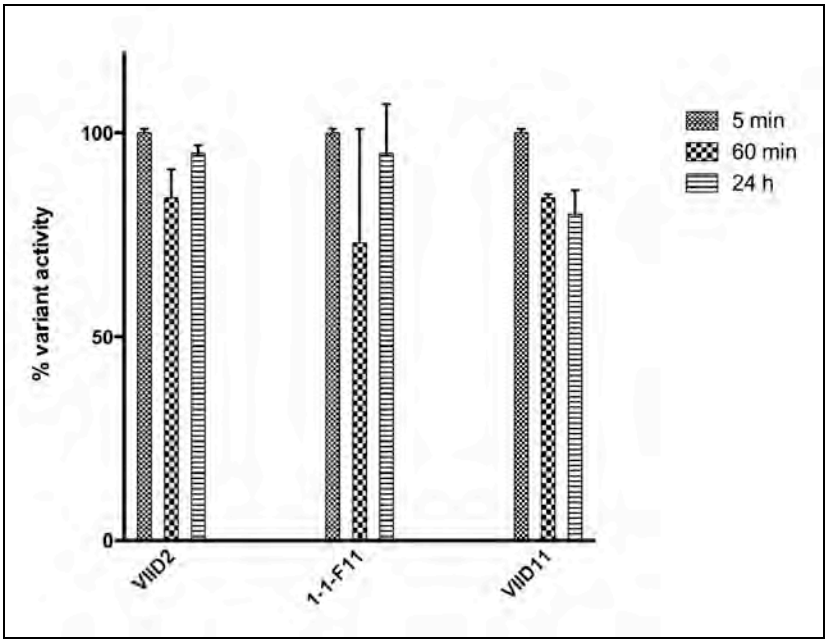

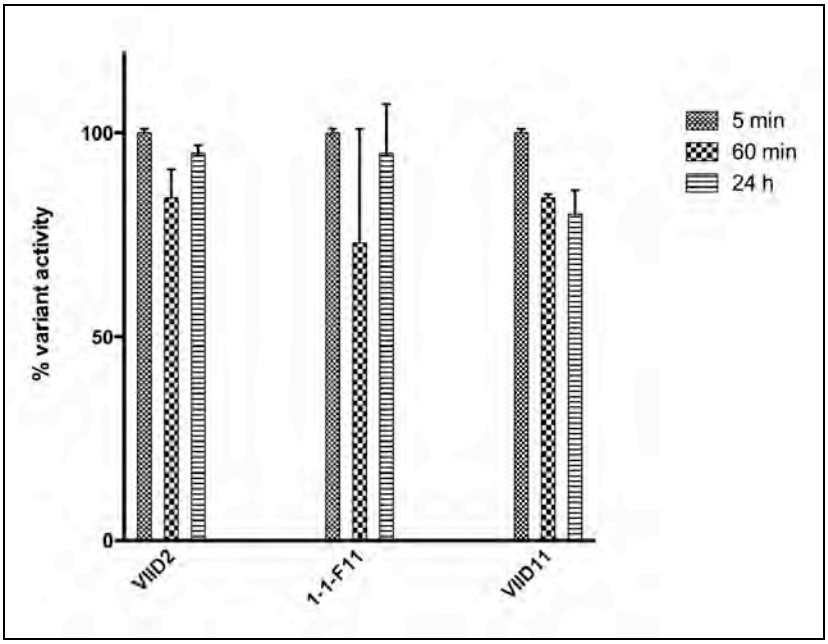

Figure 6. *Ex-vivo* stability of PON1 variants in human whole blood.

Upper panel: assayed by monitoring the protection of blood ChE activity against GF inhibition. 100% corresponds to 41-45% residual activity of blood ChE.

Lower panel: Evaluated by determination of PON1 residual activity using the GF surrogate CMP-coumarin.